**Iğdır Üniversitesi Fen Bilimleri Enstitüsü Dergisi, 12(4): 2188 - 2198, 2022**
**Journal of the Institute of Science and Technology, 12(4): 2188 - 2198, 2022**
**ISSN: 2146-0574, eISSN: 2536-4618**

**Fizik / *Physics*** **DOI: 10.21597/jist.1160050**

**Araştırma Makalesi / *Research Article***

**Geliş tarihi / *Received*: 10.08.2022** **Kabul tarihi / *Accepted*: 24.08.2022**

**Atıf İçin:** Şen Yüksel B, 2022. Meta-Siyanobenzil-Sübstitüentli NHC İçeren Yeni Pd(II)$PPh_3$ Kompleksi: Kristal Yapı ve Hesaplamalı Çalışmalar. Iğdır Üniversitesi Fen Bilimleri Enstitüsü Dergisi, 12(4): 2188 - 2198.

**To Cite:** Şen Yüksel B, 2022. New Pd(II)$PPh_3$ Complex Bearing Meta-Cyanobenzyl-Substituted NHC: Crystal Structure and Computational Studies. Journal of the Institute of Science and Technology, 12(4): 2188 - 2198.

# Meta-Siyanobenzil-Sübstitüentli NHC İçeren Yeni Pd(II)$PPh_3$ Kompleksi: Kristal Yapı ve Hesaplamalı Çalışmalar

Betül ŞEN YÜKSEL

**ÖZET:** Meta-siyanobenzil sübstitüentli NHC ve trifenilfosfin içeren paladyum(II) bileşiğinin kristal yapısı, tek kristal XRD yöntemi ile belirlendi. Moleküler geometrinin optimize hali, GEN baz seti kullanılarak DFT/B3LYP hibrit fonksiyonel yöntemi yardımıyla araştırılmıştır. Enerji aralığını hesaplamak ve yumuşaklık, sertlik, kimyasal potansiyel ve elektronegatiflik gibi bazı moleküler özellikleri belirlemek için HOMO ve LUMO analizleri kullanıldı. Ayrıca, hiperkonjugatif etkileşimlerden kaynaklanan molekül stabilitesi ve yük delokalizasyonu, doğal bağ orbital analizinden yararlanılarak gerçekleştirilmiştir. DFT yöntemi ile atomik yük analizi de yapılmıştır.

**Anahtar Kelimeler:** N-heterosiklik karbenler, kristal yapı, DFT

# New Pd(II)$PPh_3$ Complex Bearing Meta-Cyanobenzyl-Substituted NHC: Crystal Structure and Computational Studies

**ABSTRACT:** Crystal structure of palladium(II) complex containing meta-cyanobenzyl substituted NHC and triphenylphosphine were established by single-crystal XRD method. The molecular geometry in optimized form has been studied based on DFT/B3LYP hybrid functional method using the GEN basis set. The HOMO and LUMO analyses are used to compute the energy gap and to determine a number of molecular properties including softness, hardness, chemical potential, and electronegativity. Besides, the molecular stability due to hyperconjugative interactions and charge delocalization have been executed benefiting from the natural bond orbital analysis. Also, atomic charge analysis was conducted by the DFT method.

**Keywords:** N-heterocyclic carbenes, crystal structure, DFT

Betül ŞEN YÜKSEL (**Orcid ID:** 0000-0001-7846-8090), Dokuz Eylul University, Faculty of Science, Physics Department, Tınaztepe Campus, Buca, İzmir, Türkiye

**Sorumlu Yazar/*Corresponding Author***: Betül ŞEN YÜKSEL, e-mail: betul.sen@deu.edu.tr

## INTRODUCTION

N-heterocyclic carbenes (NHCs) were discovered almost five decades ago by the works of Wanzlick (Wanzlick and Schönherr, 1968) and Öfele (Öfele, 1968) independent from each other as an unstable and non-isolable form. After their seminal works, Arduengo et al. (Arduengo et al., 1991) reported the synthesis of stable NHC compounds which could also be stored and isolated. These stable NHCs have a strong coordinating ability with the majority of the transition metals due to their unique peculiarities such as strong σ-donor, poor π-acceptor, tunable steric, and electronic properties (Jafarpour and Nolan, 2000; Hu et al. 2004; Cavallo et al, 2005; Dragutan, 2007; Velazquez and Verpoort, 2012). These transition metal–NHC complexes have a prominent place in many fields of chemistry such as organometallics, organocatalysis, pharmacology, and biochemistry. For instance, Pd-based NHC complexes constitute an important class of metal-NHC complexes due to a number of peculiar properties including biological activities (Dahm et al, 2015; Akkoç et al., 2017) and catalytic properties (Gök et al., 2018; Erdoğan et al., 2018). Their catalytic activities were examined in a wide variety of organic transformations including C-C cross-coupling reactions of Suzuki-Miyaura (Benhamou et al., 2014), Sonogashira (Bhojane et al., 2017), Hiyama (Osińska et al., 2016), Mizoroki–Heck (Lin et al., 2013), and Negishi (Cinderella et al., 2017). Also, Pd-catalyzed cross-coupling reactions are one of the techniques with a wide area of use for the synthesis of sensitive chemicals. (Aravinda et al., 2013). Although electron-rich phosphine ligands are effectively used in these reactions, it is generally not possible to synthesize them in a clear-cut process due to the need for high-cost features and sensitivity to air and moisture. On the other hand, as a commonly used variety of phosphine ligands, triphenylphosphine is cheap but it offers low activity in catalytic reactions (Valentine and Hillhouse, 2003). However, $PPh_3$ is a good candidate since it exhibits resistance to air, low cost, and commercial accessibility (Guram and Buchwald, 1994). Due to their above-mentioned superior performance and beneficial properties, NHCs become promising alternative ligands against phosphines (Zhong et al., 2017; Erdemir et al., 2019). Furthermore, in recent years, the Pd-based mixed-ligand complexes from NHC and phosphine ligands were synthesized. Besides, their catalytic activities in the cross-coupling reactions were studied (Herrmann et al., 2003; Liao et al., 2009) and the catalytic activities in the Sonogashira reactions have also been published in the literature (Boubakri et al., 2017; Dehimat et al., 2018).

The palladium-based complexes with NHC ligands attract significant attention not only from an academic point of view but also for technological and medical purposes as candidate materials. Therefore, in the present article, we aim to describe the structural characterization of NHC and triphenylphosphine substituted mixed ligand palladium(II) complex. We used the single-crystal X-ray diffraction technique to analyze the molecular structure of the Pd-NHC complex. Another significant purpose of this paper is to present a detailed picture of the molecular geometry and HOMO–LUMO energies of the complex. Furthermore, the calculation results extracted by density functional theory (DFT) have been compared with the experimental findings regarding the molecular structure. We have also applied natural bond orbital (NBO) analysis to investigate the stability of the molecule emerging from charge delocalization and hyperconjugative interactions.

## MATERIALS AND METHODS

### X-ray Study

The X-ray diffraction study of the title complex was collected using Rigaku-Oxford Xcalibur diffractometer with an Eos CCD area detector. $\text{CrysAlis}^{\text{Pro}}$ program ($\text{CrysAlis}^{\text{Pro}}$, 2015) has also been used to collect and reduce the data, as well as to handle the cell refinement. The structure was solved by the SHELXT (Sheldrick, 2015) and refined with the help of the SHELXL (Sheldrick, 2015) program. These calculations are carried out under the OLEX2 system (Dolomanov et al., 2009). To handle the geometric calculations, we have utilized the PLATON package (Spek, 2003; Spek, 2009). Table 1 contains details of the crystallographic data and some parameters of refinement.

**Table 1.** Crystal data and experimental details for the title compound

| | |
|---|---|
| Formula | $C_{42}H_{33}Br_2Cl_2N_4PPd$ |
| Formula weight | 961.81 |
| Temperature (K) | 150.01(10) |
| Crystal system; space group | Triclinic; *P-1* |
| a; b; c (Å) | 9.1220(3); 14.6290(6); 16.0967(8) |
| α; β; γ (°) | 107.469(4); 102.564(3); 92.195(3) |
| Cell volume (Å$^3$) | 1987.48(14) |
| Z | 2 |
| $\rho_{calc}$ (g/cm$^3$) | 1.607 |
| F(000) | 956.0 |
| μ (mm$^{-1}$) | 2.688 |
| Crystal size (mm$^3$) | 0.286 × 0.203 × 0.073 |
| Radiation/Wavelength (Å) | MoK$_\alpha$/0.71070 |
| Reflections collected | 11257 |
| Data/restraints/parameters | 6945/12/469 |
| Final R indeces [I≥2σ(I)] | $R_1$= 0.0484, w$R_2$= 0.1120 |
| Final R indeces [all data] | $R_1$= 0.0629, w$R_2$= 0.1203 |
| GOOF on F$^2$ | 1.042 |
| Largest diff. Peak/hole (e Å$^{-3}$) | 1.21/-1.70 |

### Computational Procedure

All calculations were done using Gaussian 09 program package (Frisch et al., 2010) and Gauss–View6 molecular visualization (Dennington et al., 2016) using Becke's three-parameter hybrid and Lee-Yang-Parr correlation functional (B3LYP) (Lee et al., 1988; Becke, 1993). The molecular geometry of the complex was optimized at the GEN basis set. The GEN keyword provides user-specified basis sets which are different basis sets for different atoms in the same molecule in a Gaussian calculation. Hence, we used LANL2DZ for the Pd atom whereas, for C, N, P, Br, and H atoms, optimization and single-point calculations were performed using 6-31G and 6-311G(d,p), respectively. NBO calculations were performed utilizing the NBO 6.0 program (Glendening et al., 2013) under the Gaussian 09W package. Using NBO analysis results, orbital decomposition analysis was also performed by means of the AOMix package program (Gorelsky et al., 2006).

## RESULTS AND DISCUSSION

### Structural Definition of Complex

The molecular structure of the title complex is presented in Figure 1. The palladium atom is in an approximately square planar environment, coordinated by the carbon atom of NHC, the P atom of the triphenylphosphine group, and two bromine atoms in a *cis* configuration.

As seen in Table 2, the bond angles surrounding the Pd atom of the compound are closer to 180˚ which is an expected value for a perfect square-planar coordination arrangement. The Pd atom lies 0.038 (1) Å out of the coordination plane composed of atoms C1, P1, Br1, and Br2. The benzimidazole ring makes a dihedral angle of 76.45(10)° with the mean plane containing $PdBr_2CP$.

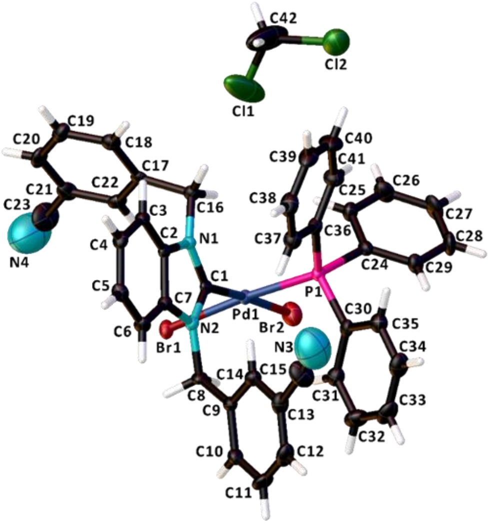

**Figure 1.** The molecular structure with the scheme of the atom labeling of the title compound. Thermal ellipsoids enclose 40% of the electron density

The bond angles and lengths in the benzimidazole ring are in usual values and they agree well with the reported Pd(II) complexes in the literature (Gökçe et al., 2006; Sarı et al.,2017; Aktaş et al., 2018; Bal et al., 2021). The two Pd–Br bond distances are almost the same as each other. These metal-ligand bond lengths are within the expected range compared to the values of known Pd(II) complexes (Özdemir et al., 2011). The Pd–C$_{(\mathrm{carbene})}$ bond length [1.995(5) Å] is slightly shorter than bond distances in the *trans* Pd(II) structures (Caló et al., 2000; Huynh et al., 2005; Özdemir et al., 2011; Sarı et al.,2017) indicating the presence of relatively strong bonded NHC ligands to the Pd atom in the *cis* form. As can be seen from the angles around the phosphorus atom (Table 2), the phosphorus atom presents distorted tetrahedral geometry. Likewise, the bond length of Pd–P falls in the range reported for related palladium(II) complexes (Asma et al., 2006; Aktaş et al., 2018; Aktaş et al., 2019). The two carbonitrile groups occupy meta positions on the benzene rings which have typical C≡N triple bonds with the C15≡N3 [C23≡N4] bond lengths of 1.091(12) Å [1.038(13) Å] and the C13–C15≡N3 [C21–C23≡N4] bond angles of 171.5(10)° [175.8(12)°].

Regarding the crystal structure, C11 atom acts as a hydrogen bond donor to the N4 atom of an inversion-related molecule, producing an $R_2^2(28)$ hydrogen-bonded dimer through the C11–H11···N4 hydrogen bond. These dimer linkages are held together by intermolecular C18–H18···Br2 hydrogen bonds and create one-dimensional chains through the [100] direction. Since each ring in the molecule is considered as a separate π system in PLATON analysis, π···π interaction analysis indicates that there are many π···π interactions in the crystal structure. If the distance between the centroids of the overlapping rings is less than 3.8 Å which corresponds to the maximum separation value for π···π interactions, a remarkable π···π interaction within the crystal structure can be mentioned (Janiak, 2000). Therefore, there exists a sole ring···ring interaction [Cg2···Cg2$^{iii}$=3.642(3) Å, inter-planar distance=-3.381(2) Å, slippage=1.354 Å, α=0.0(3)$^{o}$, symmetry code: (*v*) 1-x,1-y,-z. Cg2 is the centroid of the aromatic ring (C2–C7)] contributing to the stacking of the molecule.

Furthermore, there are two intermolecular C–H·ring interactions participating in the crystal structure stability. The molecules are also involved in a cyclic intramolecular C14–H14···N2 hydrogen bond which generates S(5) ring motifs as a five-membered N2–C8–C9–C14–H14 (Bernstein et al., 1995). The stacking of the molecules by dint of these hydrogen bonds and the intermolecular interactions is illustrated in Figure 2, and details are given in Table 3.

**Table 2.** Chosen bond lengths and angles for the present compound

| Geometric parameters | Experimental (X-ray) | Calculated B3LYP | Geometric parameters | Experimental (X-ray) | Calculated B3LYP |
|---|---|---|---|---|---|
| Bond lengths (Å) | | | | | |
| Pd1–Br1 | 2.4858(7) | 2.5417 | N1–C1 | 1.354(6) | 1.3700 |
| Pd1–Br2 | 2.4637(7) | 2.5348 | N1–C2 | 1.403(7) | 1.4094 |
| Pd1–P1 | 2.2815(14) | 2.4302 | N2–C1 | 1.348(7) | 1.3743 |
| Pd1–C1 | 1.995(5) | 2.0263 | N2–C7 | 1.401(6) | 1.4093 |
| P1–C24 | 1.818(6) | 1.8868 | N3–C15 | 1.091(12) | 1.1748 |
| P1–C30 | 1.821(5) | 1.8888 | N4–C23 | 1.038(13) | 1.1739 |
| P1–C36 | 1.830(5) | 1.8929 | C2–C3 | 1.386(7) | 1.4071 |
| Bond angles (°) | | | | | |
| Br1–Pd1–Br2 | 90.28(2) | 91.70 | C30–P1–Pd1 | 109.37(19) | 115.69 |
| Br1–Pd1–P1 | 175.52(4) | 177.62 | C30–P1–C36 | 104.0(3) | 103.21 |
| P1–Pd1–Br2 | 90.09(4) | 87.93 | C36–P1–Pd1 | 118.08(18) | 114.82 |
| Br1–Pd1–C1 | 87.89(14) | 82.61 | N2–C1–N1 | 107.1(4) | 106.34 |
| Br2–Pd1–C1 | 177.05(15) | 174.16 | N1–C1–Pd1 | 127.0(4) | 127.53 |
| C1–Pd1–P1 | 91.55(15) | 97.80 | N2–C1–Pd1 | 125.9(4) | 125.67 |
| C24–P1–Pd1 | 113.87(19) | 113.12 | C25–C24–P1 | 118.1(4) | 119.32 |
| C24–P1–C30 | 107.1(2) | 106.42 | C31–C30–P1 | 119.7(4) | 119.21 |
| C24–P1–C36 | 103.5(3) | 102.19 | C37–C36–P1 | 118.3(4) | 119.96 |

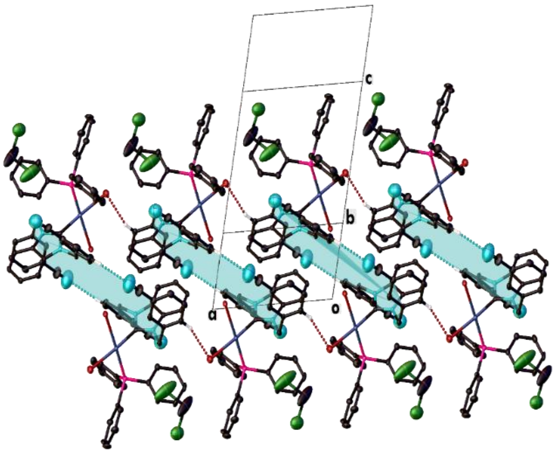

**Figure 2.** A portion of the crystal structure of the title compound which shows the formation of cyclic R ring motifs (painted in turquoise) formed by intermolecular C–H···N hydrogen bonds, as well as the arrangement of these motifs connected via intermolecular C–H···Br hydrogen bonds (the dotted red lines) along the *a*-axis. H atoms those not contribute to interactions are not displayed

**Table 3.** Hydrogen bonds and other weak interactions for the title complex (Å, °)

| *D* – H ··· *A* | *D* – H | H ··· *A* | *D* ··· *A* | *D* – H ··· *A* |
|---|---|---|---|---|
| C14–H14···N2 | 0.93 | 2.53 | 2.885(8) | 103 |
| C11–H11··· N4$^{i}$ | 0.93 | 2.52 | 3.349(15) | 150 |
| C18–H18···Br2$^{ii}$ | 0.93 | 2.83 | 3.726(6) | 162 |
| C6–H6···Cg1$^{iii}$ | 0.93 | 2.80 | 3.570(6) | 141 |
| C26–H26···Cg1$^{iv}$ | 0.93 | 2.72 | 3.580(7) | 153 |

Symmetry codes:(*i*) -x,1-y,-z; (*ii*) 1+x,y,z; (*iii*) 1-x,1-y,-z; (*iv*) - 1-x,1-y,1-z. Cg1 denotes the centroid of the (C17–C22) ring

## Molecular Geometry

The starting geometry gathered from the X-ray structure study was utilized for the theoretical investigation of the structure, then the optimization of molecular geometry was performed via DFT using the B3LYP hybrid functional in the ground state (Figure 3a). Some optimized parameters are given in Table 2 and compared with the corresponding experimental values using two different methods. First of them, accounted for the comparison of theoretical and experimental values for geometric parameters is the root mean square error (RMSE) which was put forth by Palafox (Palafox, 2018). The RMSE values are obtained as 0.038 Å for bond length whereas they are found as 1.69° for bond angle. Secondly, the

RMSE value resulting from the overlapping of molecular frameworks obtained by both X-ray determination and theoretical analysis is found to be 0.863 Å. Figure 3b shows that experimental and theoretical structures perfectly overlap with each other around the metal center. However, in the $PPh_3$ moiety, we can observe a remarkable discrepancy. Note that the reason for general deviation in results is that in the X-ray study we consider the inter- and intra-molecular forces in the solid state whereas those forces are neglected in the calculations. These results indicate that the geometry of the compound is neatly realized by the DFT/B3LYP calculation.

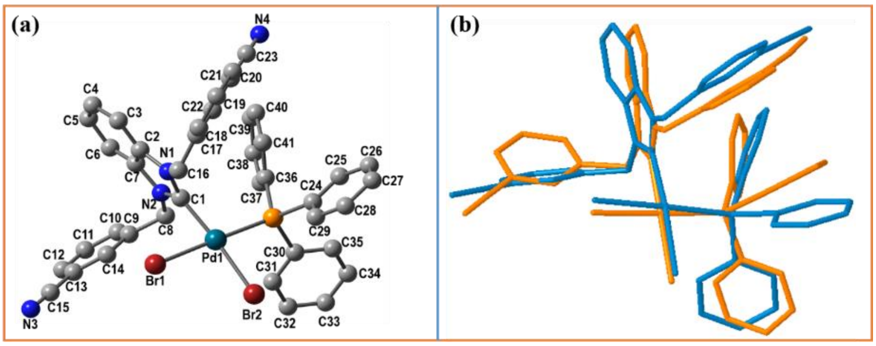

**Figure 3.** (a) The optimized structures of the complex. (b) Atom–by–atom superimposition of the theoretical structure (blue) on the experimental structure (orange) for the compound

## Frontier Molecular Orbital Analysis

HOMO and LUMO orbitals are major molecular orbitals of the molecule in which chemical reactions take place. The HOMO and LUMO energy characteristics are descriptive of the donor-acceptor characteristics of the molecule. According to the orbital energy calculations, we obtain E(gap)= E(LUMO)-E(HOMO) = (-2.398)-(-5.832) =3.434 eV which corresponds to a moderately lower energy gap indicating a more polarizable molecule (Abbas et al, 2016) and represents large efficient electrical activity. In this regard, our results yield; electronegativity (χ) 4.115 eV, chemical hardness(η) 1.717 eV, chemical potential (μ) -4.115 eV, electrophilicity index (ω) 4.931 eV.

Estimation of the most reactive position in the π-electron distribution in conjugated systems can be done with the help of Frontier electron density. Figure 4 demonstrates HOMO and LUMO orbitals. As expected, HOMO is localized around Br atoms, but LUMO is spread around the Pd atom and its neighbor atoms. The decomposition of HOMO and LUMO from atomic orbitals is calculated as follows [37,38]. HOMO: 16.9%pX(Br1) + 16.1%pz(Br1) + 10.0%pz(Br1) + 9.8%px(Br1) + 7.5%py(Br2); LUMO: 13.0%d-1(Pd1) + 11.8% d+1(Pd1) + 9.5% d+2(Pd1).

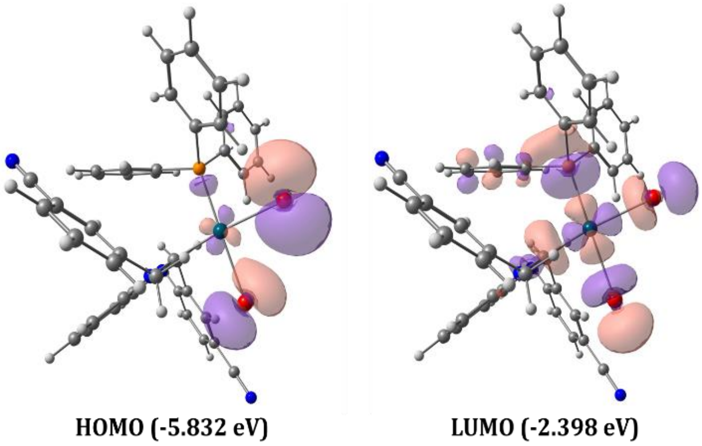

**Figure 4.** Molecular orbital surfaces and energy levels for the LUMO and HOMO of the title compound

To determine the contributions to the complex from the metal atom and neighbor groups, the complex is separated into four fragments, Pd (1), Br atoms (2), TPP group (3), and the remaining part (4). HOMO and LUMO decomposition of the frontier molecular orbitals of these fragments are: HOMO:56.4%($2_L$) + 14.8%($2_{H-1}$) + 9.4%($2_H$) and LUMO:14.5%($4_H$) + 12.4%($3_H$) + 12.1%($2_L$) + 11.5%($1_{H-4}$). In this presentation, (1), (2), (3), and (4) denote the fragments, and the subscripts H, H-1, H-4, and L show HOFO, HOFO-1, HOFO-4, and LUFO of the corresponding fragment. Since these fragments are not molecules, just fragments, these frontier orbitals are called HOFO and LUFO (highest occupied and lowest unoccupied fragment orbitals, respectively).

## Atomic Charge Analysis

Calculated atomic charges are of great importance for calculations in quantum mechanics. In this regard, the Mulliken Population Analysis (MPA) and Natural Population Analysis (NPA) with B3LYP based on 6-311G(d,p) give the following charge distributions of Pd and neighbor atoms to metal. Mulliken charges: Pd1 -0.34, Br1 -0.26, Br2 -0.28, C1 0.22, P1 0.89. Natural Population charges: Pd1 0.40, Br1 -0.50, Br2 -0.54, C1 0.30, P1 1.0. In particular, the difference in the metal atom charge can be noticed. The main reason for this difference is that while MPA is sensitive to the basis set, NPA is not. In this manner, we can conclude that NPA charges are more reasonable. Due to NPA charges, the partial charges of metal and carbene are close to each other.

## NBO Analysis

The NBO analysis is performed to study the charge transfer between the localized bonds and lone pairs. NBO analysis was performed to enlighten the charge transfer interaction in the bonds and lone pairs, for the complex at the B3LYP/6-311G(d,p) level. For the interaction energy, the off-diagonal NBO Fock matrix elements F(i,j) are given. We used the second-order perturbation method to perform this calculation (Foster and Weinhold, 1980; Glendening et al., 2013; Weinhold et al., 2016). The extra-valence-shell Rydberg ($RY^*$) orbitals, valence anti-bonds ($BD^*$), and unoccupied valence nonbonding ($LP^*$) are covered by the non-Lewis set. With the occupancy of these NBOs (Meenatchi and Meenakshisundaram, 2015), it is possible to quantify the deficiency of the Lewis-type NBOs for the representation of the density matrix. The delocalization energy $\Delta E_{ij}$ can be computed using $E(2)=\Delta E_{ij}= q_i F(i,j)^2/(\varepsilon_j-\varepsilon_i)$; where E(2) stands for the hyperconjugation interaction, $q_i$ denotes the occupancy of the Lewis type orbital. $\varepsilon_j$ and $\varepsilon_i$ respectively correspond to the donating and accepting orbital energies (Foster and Weinhold, 1980; Weinhold et al., 2016). A remarkable contribution to stabilization energy of $n \rightarrow \sigma^*$ (P1 → Pd1-Br2) 72.35 kcal/mol and $n \rightarrow \pi^*$ (N1→ N2-C1) 70.80 kcal/mol are the largest values for lowering the perturbation energy. Besides, $\sigma \rightarrow \sigma^*$ (Pd1-C8 → Pd1-Br2) with 34.74 kcal/mol is observed. In addition, some interactions contribute ~20 kcal/mol in phenyl groups containing conjugated electrons.

## CONCLUSION

The crystal structure of the Pd(II) complex has been obtained by X-ray crystallography revealing that the complex is four-coordinated in a more or less distorted square-planar environment. To reinforce the structure of the solid-state, the molecular structure is clarified by the DFT/B3LYP with GEN basis set (LanL2DZ for Pd atom and 6.31G for the other atoms), and obtained geometric parameters are compared with the experimental observation. Most of the theoretical outcomes are consonant with the available experimental values. The computed HOMO–LUMO band gap presents a moderately lower energy gap and shows the chemical reactivity of the molecule. The molecule stability due to hyperconjugative interactions and charge delocalization have been executed benefiting from NBO analysis

## ACKNOWLEDGEMENTS

Contributions of Prof. Yetkin GÖK from İnönü University and Assoc. Prof. Muhittin AYGÜN from Dokuz Eylül University are greatly acknowledged due to the synthesis and crystallization of molecule and for the use of the Gaussian 09W software. The CCDC code of the structure is 2154988.

## REFERENCES

Abbas A, Gökce H, Bahceli S, Bolte M, Naseer MM, 2016. Solid state structural and theoretical investigations of a biologically active chalcone. Journal of Molecular Structure, 1112: 124–135.

Akkoç S, Kayser V, Özer I, Hibbs DE, Gök Y, Williams PA, Hawkins B, Lai F, 2017. New Compounds Based on a Benzimidazole Nucleus: Synthesis, Characterization and Cytotoxic Activity Against Breast and Colon Cancer Cell Lines. Journal of Organometallic Chemistry, 839: 98-107.

Aktaş A, Barut Celepci D, Gök Y, Aygün M, 2018. 2-Hydroxyethyl-Substituted Pd-PEPPSI Complexes: Synthesis, Characterization and the Catalytic Activity in the Suzuki-Miyaura Reaction for Aryl Chlorides in Aqueous Media. ChemistrySelect, 3: 9974–9980.

Aktaş A, Celepci DB, Gök Y, Aygün M, 2018. 2-Hydroxyethyl-Substituted (NHC)Pd(II)PPh3 Complexes: Synthesis, Characterization, Crystal Structure and Its Application on Sonogashira Cross-Coupling Reactions in Aqueous Media. ChemistrySelect, 3(39): 10932–10937.

Aktaş A, Erdemir F, Barut Celepci D, Gök Y, Aygün M, 2019. Mixed phosphine/N-heterocyclic carbene–palladium complexes: synthesis, characterization, crystal structure and application in the Sonogashira reaction in aqueous media. Transition Metal Chemistry, 44: 229-236.

Aravinda RP, Babul RA, Ramachandra RG, Subbarami RN, 2013. Suzuki–Miyaura Cross-Coupling Reaction of Naphthyl Triflate with Indole Boronic Acids Catalyzed by a Recyclable Polymer-Supported N-Heterocyclic Carbene–Palladium Complex Catalyst: Synthesis of Naphthalene-Linked Bis- Heterocycles. Journal of Heterocyclic Chemistry, 50(6): 1451-1456.

Arduengo AJ, Harlow RL, Kline M, 1991. A stable crystalline carbene. Journal of the American Chemical Society, 113(1): 361–363.

Asma M, Badshah A, Ali S, Sohail M, Fettouhi M, Ahmad S, Malik A, 2006. Synthesis, characterization of mixed ligand palladium (II) complexes of triphenylphosphine and anilines and their enzyme inhibition studies against βglucuronidase. The crystal structure of trans-dichloro-(mchloroaniline) (triphenylphosphine) palladium (II). Transition Metal Chemistry, 31: 556- 559.

Bal S, Demirci Ö, Şen B, Taslimi P, Aktaş A, Gök Y, Aygün M, Gülçin İ, 2021. PEPPSI type Pd(II)NHC complexes bearing chloro-/fluorobenzyl group: Synthesis, characterization, crystal structures, α-glycosidase and acetylcholinesterase inhibitory properties. Polyhedron, 198: 115060.

Becke AD, 1993. Density-functional thermochemistry. III. The role of exact exchange. The Journal of Chemical Physics, 98: 5648.

Benhamou L, Besnard C, Kündig EP, 2014. Chiral PEPPSI Complexes: Synthesis, Characterization, and Application in Asymmetric Suzuki–Miyaura Coupling Reactions. Organometallics, 33: 260-266.

Bernstein J, Davis RE, Shimoni L, Chang NL, 1995. Patterns in Hydrogen Bonding: Functionality and Graph Set Analysis in Crystals. Angewandte Chemie International Edition in English, 34(15): 1555-1573.

Bhojane JM, Jadhav VG, Nagarkar JM, 2017. Pd(NHC)PEPPSI-diazonium salts: an efficient blend for the decarboxylative Sonogashira cross coupling reaction. New Journal of Chemistry, 41(14): 6775-6780.

Bondi A, 1964. van der Waals Volumes and Radii. The Journal of Physical Chemistry, 68(3): 441-451.

Boubakri L, Yasar S, Dorcet V, Roisnel T, Bruneau C, Hamdi N, Ozdemir I, 2017. Synthesis and catalytic applications of palladium N-heterocyclic carbene complexes as efficient pre-catalysts for Suzuki–Miyaura and Sonogashira coupling reactions. New Journal of Chemistry, 41(12): 5105-5113.

Caló V, Sole RD, Nacci A, Schingaro E, Scordari F, 2000. Synthesis and Crystal Structure of Bis(2,3-dihydro-3-methylbenzothiazole-2-ylidene)palladium(II) Diiodide: The First Palladium Complex with Benzothiazole Carbene Ligands Suitable for Homogeneous Catalysis. European Journal of Organic Chemistry, 869–871.

Cavallo L, Correa A, Costabile C, Jacobsen H, 2005. Steric and electronic effects in the bonding of N-heterocyclic ligands to transition metals. Journal of the Organometallic Chemistry, 690: 5407-5413.

Cinderella AP, Vulovic B, Watson DA, 2017. Palladium-Catalyzed Cross-Coupling of Silyl Electrophiles with Alkylzinc Halides: A Silyl-Negishi Reaction. Journal of the American Chemical Society, 139(23): 7741-7744.

CrysAlis$^{Pro}$ Software System, Rigaku Corporation, Oxford, UK, 2015. Version 1.171.38.43.

Dahm G, Bailly C, Karmazin L, Bellemin-Laponnaz S, 2015. Synthesis, structural characterization and in vitro anti-cancer activity of functionalized N-heterocyclic carbene platinum and palladium complexes. Journal of Organometallic Chemistry, 794: 115–124.

Dehimat ZI, Yaşar S, Tebbani D, Özdemir İ, 2018. Sonogashira cross-coupling reaction catalyzed by N-heterocyclic carbene-Pd(II)-PPh3 complexes under copper free and aerobic conditions. Inorganica Chimica Acta, 469: 325-334.

Dennington R, Keith TA, Millam JM, 2016. GaussView, Version 6, Semichem Inc. Shawnee Mission. KS.

Dolomanov OV, Bourhis LJ, Gildea RJ, Howard JAK, Puschmann H, 2009. OLEX2: A complete structure solution, refinement and analysis program. Journal. Applied Crystallography, 42: 339-341.

Dragutan V, Dragutan I, Delaude L, Demonceau A, 2007. NHC-Ru complexes-Friendly catalytic tools for manifold chemical transformations. Coordination Chemistry Reviews, 251(5-6): 765-794.

Erdemir F, Barut Celepci D, Aktaş A, Gök Y, 2019. 2-hydroxyethyl-substituted (NHC)PdI$_2$ (pyridine) (Pd-PEPPSI) complexes: synthesis, characterization and the catalytic activity in the sonogashira cross-coupling reaction. ChemistrySelect, 4: 5585-5590.

Erdoğan H, Aktaş A, Gök Y, Sarı Y 2018. N-Propylphthalimide-substituted bis-(NHC)PdX$_2$ complexes: synthesis, characterization and catalytic activity in direct arylation reactions. Transition Metal Chemistry, 43: 31-37.

Foster JP, Weinhold F, 1980. Natural hybrid orbitals. Journal of the American Chemical Society, 102(24): 7211-7218.

Frisch MJ, Trucks GW, Schlegel HB, Scuseria GE, Robb MA, Cheeseman JR, Scalmani G, Barone V, Petersson, GA, Nakatsuji H, Li X, Caricato M, Marenich A, Bloino J, Janesko B G, Gomperts R, Mennucci B, Hratchian HP, Ortiz JV, Izmaylov AF, Sonnenberg JL, Williams-Young D, Ding F, Lipparini F, Egidi F, Goings J, Peng B, Petrone A, Henderson T, et al., 2010. Gaussian 09 Revision B.01. Gaussian, Inc. Wallingford CT.

Glendening ED, Landis CR, Weinhold F, 2013. Nbo 6.0: Natural bond orbital analysis program. Journal of Computational Chemistry, 34: 1429-1437.

Glendening E D, Badenhoop JK, Reed AE, Carpenter JE, Bohmann JA, Morales CM, Landis CR, Weinhold F, 2013. NBO 6.0. Theoretical Chemistry Institute, University of Wisconsin, Madison, WI, http://nbo6.chem.wisc.edu/

Gorelsky SI, Ghosh S, Solomon EI, 2006. Mechanism of $N_2O$ Reduction by the $\mu_4$-S Tetranuclear $Cu_Z$ Cluster of Nitrous Oxide Reductase. Journal of the American Chemical Society, 128(1): 278–290.

Gök Y, Aktas A, Erdoğan H, Sarı Y, 2018. New 4-vinylbenzyl-substituted bis(NHC)-Pd(II) complexes: Synthesis, characterization and the catalytic activity in the direct arylation reaction. Inorganica Chimica Acta, 471: 735-740.

Gökçe AG, Gülcemal S, Aygün M, Çetinkaya B, Büyükgüngör O, 2006. trans-Bis[1-benzyl-3-(2,3,4,5,6-pentafluorobenzyl)benzimidazol-2-ylidene]dibromopalladium(II). Acta Crystallographica Section C Crystal Structure Communications. 62(11): m535–m537.

Guram AS, Buchwald SL, 1994. Palladium-Catalyzed Aromatic Aminations with in situ Generated Aminostannanes. Journal of the Americal Chemical Society, 116:7901-7902.

Herrmann WA, Öfele K, Preysing D, Schneider SK, 2003. Phospha-palladacycles and N-heterocyclic carbene palladium complexes: efficient catalysts for CC-coupling reactions. Journal of Organometallic Chemistry, 687(2): 229–248.

Hu X, Castro-Rodriguez I, Olsen K, Meyer K, 2004. Group 11 Metal Complexes of N-Heterocyclic Carbene Ligands: Nature of the Metal-Carbene Bond. Organometallics, 23: 755-764.

Huynh HV, Ho JH, Neo TC, Koh LL, 2005. Solvent-controlled selective synthesis of a trans-configured benzimidazoline-2-ylidene palladium(II) complex and investigations of its Heck-type catalytic activity. Journal of Organometallic Chemistry, 690: 3854–3860.

Jafarpour L, Nolan SP, 2000. Transition-metal systems bearing a nucleophilic carbene ancillary ligand: from thermochemistry to catalysis. Advances in Organometallic Chemistry, 46: 181-222.

Janiak C, 2000. A critical account on π-π stacking in metal complexes with aromatic nitrogen-containing ligands. Journal of the Chemical Society, Dalton Transactions, 21: 3885–3896.

Lee C, Yang W, Parr RG, 1988. Development of the Colle-Salvetti correlation-energy formula into a functional of the electron density. Physical Review, 37: 785.

Liao CY, Chan KT, Tu CY, Chang YW, Hu CH, Lee HM, 2009. Robust and electron-rich cis-palladium(II) complexes with phosphine and carbene ligands as catalytic precursors in Suzuki coupling reactions. Chemistry-A European Journal, 15: 405-417.

Lin YC, Hsueh HH, Kanne S, Chang LK, Liu FC, Lin IJB, Lee GH, Peng SM, 2013. Efficient PEPPSI-Themed Palladium N-Heterocyclic Carbene Precatalysts for the Mizoroki–Heck Reaction. Organometallics, 32: 3859-3869.

Palafox MA, 2018. DFT computations on vibrational spectra: Scaling procedures to improve the wavenumbers. Physical Sciences Reviews, 3: 1-30.

Osińska M, Gniewek A, Trzeciak AM, 2016. Suzuki–Miyaura and Hiyama coupling catalyzed by PEPPSI-type complexes with non-bulky NHC ligand. Journal of Molecular Catalysis A: Chemical, 418-419: 9-18.

Öfele K, 1968. 1,3-Dimethyl-4-imidazolinyliden-(2)-pentacarbonylchrom ein neuer übergangsmetall-carben-komplex. Journal of Organometallic Chemistry, 12(3): 42-43.

Özdemir İ, Arslan H, Demir S, VanDerveer D, Çetinkaya B, 2011. Synthesis, characterization and catalytic properties of cis-dibromo{1,1′-di[3,4,5-trimethoxybenzyl]-3,3′-butylenedibenzimidazol-2,2′-diylidene}palladium (II). Inorganic Chemistry Communications, 14(5): 672–675.

Sarı Y, Aktaş A, Barut Celepci D, Gök Y, Aygün M, 2017. Synthesis, Characterization and Crystal Structure of New 2-Morpholinoethyl-Substituted Bis-(NHC)Pd(II) Complexes and the Catalytic Activity in the Direct Arylation Reaction. Catalysis Letters, 147: 2340-2351.

Sheldrick GM, 2015. SHELXT-integrated space-group and crystal-structure determination. Acta Crystallographica A Foundations and Advances, A71: 3-8.

Sheldrick GM, 2015. Crystal structure refinement with SHELXL. Acta Crystallographica C Structural Chemistry, C71: 3-8.

Spek AL, 2003. Single-crystal structure validation with the program PLATON. Journal of Applied Crystallography, 36: 7-13.

Spek AL, 2009. Structure validation in chemical crystallography. Acta Crystallographica D65, 148-155.

Valentine Jr DH, Hillhouse JH, 2003. Electron-Rich Phosphines in Organic Synthesis II. Catalytic Applications. Synthesis, 16: 2437-2460.

Velazquez HD, Verpoort F, 2012. N-heterocyclic carbene transition metal complexes for catalysis in aqueous media. Chemical Society Reviews, 41(21), 7032-7060.

Wanzlick HW, Schönherr HJ, 1968. Direct Synthesis of a Mercury Salt-Carbene Complex. Angewandte Chemie International Edition in English, 7(2): 141-142.

Weinhold F, Landis CR, Glendening ED, 2016. What is NBO analysis and how is it useful? International Reviews in Physical Chemistry, 35(3): 399–440.

Zhong R, Lindhorst AC, Groche FJ, Kühn FE, 2017. Immobilization of N-Heterocyclic Carbene Compounds: A Synthetic Perspective. Chemical Reviews, 117(3): 1970–2058.